


Lifshitz transition in dirty doped topological insulator with nematic superconductivity

R. S. Akzyanov *Dukhov Research Institute of Automatics, Moscow, 127055, Russia;**Moscow Institute of Physics and Technology, Dolgoprudny, Moscow Region, 141700, Russia;**and Institute for Theoretical and Applied Electrodynamics, Russian Academy of Sciences, Moscow, 125412, Russia* (Received 12 July 2021; revised 23 September 2021; accepted 23 November 2021; published 10 December 2021)

We study the effects of the Lifshitz transition from the closed to open Fermi surface in dirty topological insulators with nematic superconductivity near the critical temperature. We solve linearized Gor'kov equations and find that the nematic superconductor with an open Fermi surface has a lower critical temperature and is more susceptible to disorder than the superconductor with the closed Fermi surface. We propose that correspondence between the critical temperature and stability against the disorder is a general feature of the superconductivity. We investigate the effects of the Lifshitz transition on the competition between superconducting phases in a topological insulator. The open Fermi surface is beneficial for the nematic order parameter Δ_4 in competition with orbital-triplet Δ_2 and disfavors nematic state over the s -wave order parameter. We study Meissner currents in both clean and dirty limits. We found that transition from closed to open Fermi surface increases anisotropy of Meissner currents. Finite disorder suppresses superconducting density stronger than critical temperature. We compare our results with existing experimental data.

DOI: [10.1103/PhysRevB.104.224502](https://doi.org/10.1103/PhysRevB.104.224502)

I. INTRODUCTION

Superconductivity in topological insulators in Bi_2Se_3 family attracts significant attention due to realization of topological odd-parity superconductivity [1,2]. Experiments on Knight shift [3], second critical field [4–6], and magnetic torque [7] show twofold symmetry of the response that is incommensurate with the crystal symmetry. Such symmetry breaking arises from nematic superconducting order parameter within E_u representation [8,9]. Unconventional nematic superconductivity gives rise to several intriguing phenomena such as surface Andreev bound states [10–12], half-quantum vortices [13,14], spin (nematic) vortices [15], spontaneous strain and magnetization [16], vestigial order [17], unconventional Higgs modes [18], and anisotropic quasiparticle interference [19,20].

The Anderson theorem [21] does not hold in general for unconventional superconductivity that results in suppression of the critical temperature T_c by the disorder [22]. In Ref. [23] it was found that proton irradiation of $\text{Nb}_x\text{Bi}_2\text{Se}_3$ decreases critical temperature with increasing density of defects. However, only a small part of scattering events contribute to the pair-breaking mechanism [23]. Excessive Cu doping of Bi_2Se_3 brings additional defects into the system that leads to a slight decrease of critical temperature with the increased doping [24,25].

In Refs. [26–29] effects of the disorder on critical temperature of nematic superconductor were studied. It was found that density disorder decreases critical temperature for the nematic order parameter. These results contradict the results of Ref. [30] where the robustness of nematic superconductivity against disorder was derived.

Superfluid density is particularly sensitive to disorder [31]. In Ref. [24] it was shown that an increase of disorder

suppresses superfluid density in a doped topological insulator. This superfluid density determines the first critical field of the superconductor and London penetration length. In Refs. [32,33] it was shown that the out-of-plane first critical field in $\text{Nb}_x\text{Bi}_2\text{Se}_3$ is much smaller than the in-plane first critical field.

The transition from closed Fermi surface to an open one is called as Lifshitz transition [34]. This transition occurs in underdoped cuprates and has a significant effect on the superconducting properties [35–37]. Lifshitz transition appears in topological insulator Bi_2Se_3 upon doping with Nb or Cu [38,39]. The appearance of this transition coincides with the emergence of superconductivity in the system [39].

In our paper, we answer the question of how Lifshitz transition affects critical temperature, stability against the disorder, and Meissner currents in a topological insulator with nematic superconductivity. This paper is organized as follows. In Sec. II we introduce the Hamiltonian of a topological insulator with nematic superconductivity and introduce a model for a Lifshitz transition. In Sec. III we solve linearized Gor'kov equations for Green's functions in a clean limit and calculate the critical temperature in case of closed and open Fermi surfaces of the normal state. In Sec. IV we calculate self-energy that arises due to scattering from the randomly distributed scalar disorder and analyze the effects of the disorder on the critical temperature. In Sec. V we discuss general properties of the robustness of the superconducting states against disorder. We establish a general connection between critical temperature and stability against disorder and tie it with the conception of superconducting fitness. In Sec. VI we calculate superfluid density in clean and dirty limits and show how Lifshitz transition affects the anisotropy of the first critical field. In the Discussion section, we compare our results with experimental results and other works within the field.

II. MODEL

We give a short summary of derivation of the Hamiltonian of the normal state of topological insulators from Refs. [40,41]. Crystal structure of Bi_2Se_3 consists of layers of Bi and Se. Five such layers form one quintuple layer. These quintuple layers interact weakly through van der Waals forces. Thus, interactions within quintuple layer are the strongest ones. In each quintuple layer the central layer consists of Se atoms that are sandwiched by Bi layers and Se layers are outermost. Outermost orbitals of Bi ($6s^26p^3$) and Se ($4s^24p^4$) are p orbitals and we can neglect other orbitals. Hybridization between Bi and Se orbitals leads to the formation of new hybridized orbitals of bismuth (Bi and Bi^*) and selenide Se (Se^* and $\text{Se}0$). Due to the presence of inversion crystal symmetry it is convenient to consider bonding and antibonding states with definite parity. State $P1^\pm = (\text{Bi} \pm \text{Bi}^*)/\sqrt{2}$ corresponds to the bonding + or antibonding - state of Bi orbitals, state $P2^\pm = (\text{Se} \pm \text{Se}^*)/\sqrt{2}$ corresponds to the bonding + or antibonding - state of Se orbitals. Here \pm corresponds to the parity of the state. After taking into account of hybridization between Bi(Se) and $\text{Bi}^*(\text{Se}^*)$ orbitals it is found that bonding state of $P1^+$ and antibonding state of $P2^-$ are closest to the Fermi level. The crystal has a layered structure along the z direction which is different from the x or y direction. Thus, crystal field leads to energy splitting between p_z and p_x, p_y orbitals. It is found that p_z orbitals form conduction $P1^+$ and valence bands $P2^-$ prior to consideration of the spin-orbit interaction. Strong spin-orbit interaction pushes energy of $P1^+$ down and $P2^-$ up. At some value of spin-orbit interaction orbitals with opposite parity cross, which leads to band inversion. This band inversion is a signature of the topological insulator. This transition occurs at the time-reversal-invariant symmetric Γ point that is located at the center of the Brillouin zone $\Gamma(0, 0, 0)$. At this point orbitals are closest to the Fermi level. Now, low-energy effective Hamiltonian $H_N(\mathbf{k})$ can be obtained by fitting kp expansion in $(P1^+, P2^-)$ basis near the Γ point to the density functional theory (DFT) calculations [40,41]

$$H_N(\mathbf{k}) = -\mu + m\sigma_z + v\sigma_x(s_xk_y - s_yk_x) + v_zk_z\sigma_y. \quad (1)$$

Here Pauli matrices s_x, s_y, s_z act in the spin space (\uparrow, \downarrow), Pauli matrices $\sigma_x, \sigma_y, \sigma_z$ act in the space of inverted orbitals of Bi and Se atoms near the Fermi level ($P1^+, P2^-$), μ is the chemical potential, $2m$ is the value of the single-electron gap at half-filling $\mu = 0$ at Γ point ($\mathbf{k} = 0$), v is the in-plane Fermi velocity within the main ($\Gamma M, \Gamma K$) plane that is parallel to the plane of Bi and Se layers, and v_z is the Fermi velocity along the ΓZ direction that is perpendicular to the orientation of Bi and Se layers. Away from the Γ point new terms in the Hamiltonian arise that lead to k dependence of the parameters of the Hamiltonian and emergence of the hexagonal warping which will be discussed in Sec. V. It is worth to mention that linear dispersion along the z direction works well even away from the Γ point (see Ref. [41]).

The spectrum of the normal state is given by

$$E(\mathbf{k}) = -\mu \pm \sqrt{m^2 + v^2k_x^2 + v^2k_y^2 + v_z^2k_z^2}. \quad (2)$$

The closed Fermi surface forms an ellipsoid that is elongated along the z direction since $v_z < v$. This ellipsoid can

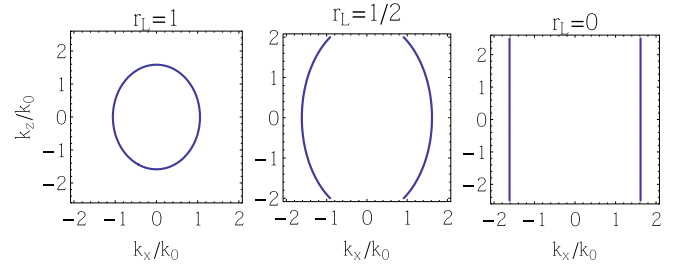


FIG. 1. Fermi surface in $(k_x/k_0, k_z/k_0)$ plane for $k_y = 0$ for different values of Lifshitz parameter r_L . Left figure corresponds to the closed Fermi surface $r_L = 1$ with $\mu = 1.5m$, central figure to corrugated cylinder $r_L = 1/2$ with $\mu = 2.8m$, right figure to cylindrical Fermi surface $r_L = 0$ with $\mu = 2.8m$ and $v_z = 0$. Here $k_0 = m/v$, upper and lower boundaries in the k_z direction show the the boundary for the first Brillouin zone. Boundary for the first Brillouin zone in the k_x direction is $c/a \sim 7$ (here a and c are lattice constants) times larger than the boundary in the k_z direction and is not shown here.

be parametrized by ellipsoid coordinates $(vk_x, vk_y, v_zk_z) = \sqrt{\mu^2 - m^2}(\cos \varphi \sin \theta, \sin \varphi \sin \theta, \cos \theta)$. In case of closed Fermi surface $\varphi \in (0, 2\pi)$ and $\theta \in (0, \pi)$.

The Lifshitz transition from closed to open Fermi surface occurs if the size of the Brillouin zone k_c becomes smaller than the Fermi momentum $v_zk_c < \sqrt{\mu^2 - m^2}$. In ellipsoid coordinates this results that angle $\theta \in (\theta_L, \pi - \theta_L)$ where $\cos \theta_L = \min(1, v_zk_c/\sqrt{\mu^2 - m^2})$. Here we introduce parameter $r_L = \cos \theta_L$ that controls the Lifshitz transition. If $r_L = 1$, then the Fermi surface is closed. In case of $r_L < 1$ the Fermi surface becomes open. Case $r_L = 0$ corresponds to the purely cylindrical Fermi surface. Fermi surface $E(\mathbf{k}) = 0$ is shown in Fig. 1 for different values of r_L . Note that the obtained Fermi surface is similar to the experimental and DFT calculated Fermi surfaces [38,39].

In our work, we suppose that electron-phonon interaction is short range and has no dependence on the Lifshitz transition. In Ref. [42] it was shown that near the Lifshitz transition electron-phonon coupling is enhanced along the $[001]$ direction. Also, electron-phonon coupling is singular along the k_z direction and isotropic in the (k_x, k_y) plane. It means that electrons with the small k_z momentum have strongest coupling. Anisotropic singular coupling $g = g(k_z)$ can be modeled by step function with the size k_c . This anisotropic coupling results in the same effects on the superconductivity as a Lifshitz transition except for the density of states $\rho(\mu)$ is unchanged.

The form of the Fermi surface has a significant impact on the density of states. We suppose that only the states near the Fermi surface contribute and calculate density of states at zero frequency as

$$\rho(\mu) = -\frac{1}{\pi} \text{Im Tr} \sum_k G_0(\omega \rightarrow +0) = \frac{r_L \mu \sqrt{\mu^2 - m^2}}{v^2 v_z \pi^2}, \quad (3)$$

where the Green's function of the normal state $G_0 = [i\omega - H_N(\mathbf{k})]^{-1}$ is

$$G_0 = \frac{-i\omega - \mu - m\sigma_z - v\sigma_x(s_xk_y - s_yk_x) - v_zk_z\sigma_y}{m^2 + v_z^2k_z^2 + v^2(k_x^2 + k_y^2) - (\mu + i\omega)^2}. \quad (4)$$

We plot the density of states as a function of doping μ in the absence and presence of the Lifshitz transition at Fig. 2.

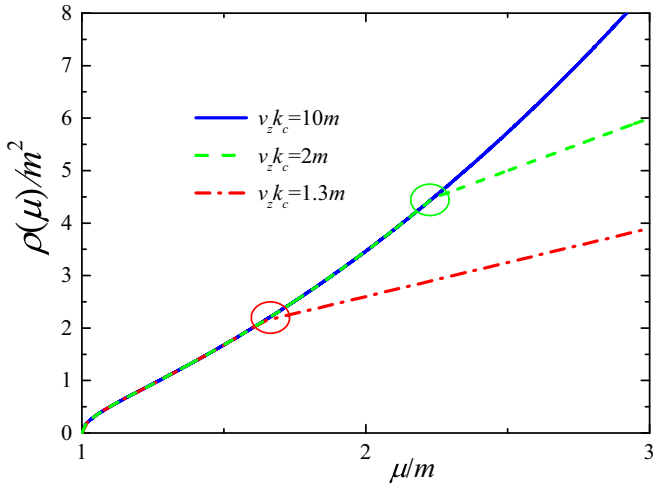


FIG. 2. Density of states $\rho(\mu)$ as a function of chemical potential μ for different values of the Brillouin zone size $v_z k_c$. Red and green circles show point of the Lifshitz transition for $v_z k_c = 1.3$ and 2 , respectively.

Increase of the chemical potential increases density of states by the square law $\rho \propto \mu^2$ for $\mu \gg m$ in case of the closed Fermi surface $r_L = 1$. After the Lifshitz transition $r_L < 1$ the density of states increases linearly with the increase of chemical potential $\rho \propto \mu$. This picture is in qualitative agreement with the density functional theory calculations: fast growth of the density of states before Lifshitz transition and slow growth after it.

We consider the system with the odd-parity order parameter within E_u representation. Such nematic order parameter couples electrons from different orbitals with the same spin and preserves time-reversal symmetry. This order parameter has a vector structure $\Delta = (\Delta_x, \Delta_y)$ that differs from other possible pairings that transforms as a scalar under rotation. In Nambu basis $(\Psi(k), i s_y \Psi^*(-k))$ doped topological insulator with superconductivity can be described by the Hamiltonian (see Ref. [43] for discussion about form of the order parameters in different basis)

$$H_{\text{BdG}}(\mathbf{k}) = H_N(\mathbf{k})\tau_z + \hat{\Delta}\tau_x, \quad (5)$$

$$\hat{\Delta} = (\Delta_x s_x + \Delta_y s_y)\sigma_y, \quad (6)$$

where Pauli matrices τ_i act in a Nambu particle-hole space.

III. GOR'KOV EQUATIONS FOR THE CLEAN CASE

We start with the Gor'kov equations in the general case in the Nambu basis $\Psi = (\Psi(k), i s_y \Psi^*(-k))$. Green's functions

can be obtained by solving Gor'kov equations

$$(i\omega - \hat{H}_{\text{BdG}})\hat{G}_0 = \hat{1}, \quad (7)$$

where Hamiltonian in Nambu space expresses as

$$i\omega - \hat{H}_{\text{BdG}} = \begin{pmatrix} i\omega - H_N(k) & -\hat{\Delta} \\ -\hat{\Delta}^\dagger & i\omega + s_y H_N^*(-k) s_y \end{pmatrix}, \quad (8)$$

and Green's function \hat{G}_0 as

$$\hat{G}_0 = \begin{pmatrix} G_{0e} & F_0 \\ \bar{F}_0 & G_{0h} \end{pmatrix}. \quad (9)$$

Here G_{0e} (G_{0h}) is the normal part of electrons (holes) and F_0 is the anomalous part of the Green's functions. The Hamiltonian of the normal state is $H_N(k)$, $\hat{\Delta}$ is the superconducting order parameter, $\omega = \pi T(2n + 1)$ is the fermionic Matsubara frequency for temperature T , and $\hat{1}$ is identity matrix. For the anomalous Green's function that is responsible for the superconducting correlations in the system we have

$$F_0 = [i\omega - H_N(k)]^{-1} \hat{\Delta} G_{0h}, \quad (10)$$

$$\bar{F}_0 = [i\omega + s_y H_N^*(-k) s_y]^{-1} \hat{\Delta}^\dagger G_{0e}. \quad (11)$$

The normal part of Green's function expresses as

$$G_{0e} = (1 - G_0 \hat{\Delta} G_0^* \hat{\Delta}^\dagger)^{-1} G_0, \quad (12)$$

$$G_{0h} = (1 - \bar{G}_0 \hat{\Delta}^\dagger G_0 \hat{\Delta})^{-1} \bar{G}_0, \quad (13)$$

where we introduce bare Green's functions of the normal state as

$$G_0 = [i\omega - H_N(k)]^{-1}, \quad (14)$$

$$\bar{G}_0 = [i\omega + s_y H_N^*(-k) s_y]^{-1}. \quad (15)$$

Near critical temperature T_c we can keep only linear in order parameter $\hat{\Delta}$ terms in the Green's functions. We consider a system with the time-reversal symmetry $s_y H_N^*(-k) s_y = H_N(k)$ that results in

$$G_{0e} = G_0, \quad G_{0h} = \bar{G}_0, \quad (16)$$

$$F_0 = G_0 \hat{\Delta} \bar{G}_0, \quad \bar{F}_0 = \bar{G}_0 \hat{\Delta}^\dagger G_0. \quad (17)$$

Note that $\bar{G}_0(\omega) = -G_0(-\omega)$. We will use these linearized in $\hat{\Delta}$ expressions for our calculations. In case of topological insulator we use Eq. (4) for G_0 . Linearized anomalous Green's functions are written as

$$F_0 = \frac{2f(k, \Delta, \omega)}{B_N},$$

$$\bar{F}_0 = -2f(k, \Delta^\dagger, -\omega)/B_N, \quad (18)$$

where

$$f(k, \Delta, \omega) = -v_z k_z \mu (\Delta_x s_x + \Delta_y s_y) + mv(k_x \Delta_x + k_y \Delta_y) s_z + v v_z k_z (k_x \Delta_y - k_y \Delta_x) \sigma_x - m\omega (\Delta_x s_x + \Delta_y s_y) \sigma_x$$

$$+ J_x s_x \sigma_y + J_y s_y \sigma_y + v\omega (k_y \Delta_x - k_x \Delta_y) \sigma_z - v_z k_z m (\Delta_x s_x + \Delta_y s_y) \sigma_z + v\mu (k_x \Delta_x + k_y \Delta_y) s_z \sigma_z,$$

$$J_x = \{ \Delta_x [m^2 - \mu^2 - \omega^2 + v^2(k_y^2 - k_x^2) - v_z^2 k_z^2] - 2v^2 k_x k_y \Delta_y \} / 2,$$

$$J_y = \{ \Delta_y [m^2 - \mu^2 - \omega^2 + v^2(k_x^2 - k_y^2) - v_z^2 k_z^2] - 2v^2 k_x k_y \Delta_x \} / 2,$$

$$B_N = [m^2 + v_z^2 k_z^2 + v^2(k_x^2 + k_y^2) - \mu^2 + \omega^2]^2 + 4\mu^2 \omega^2. \quad (19)$$

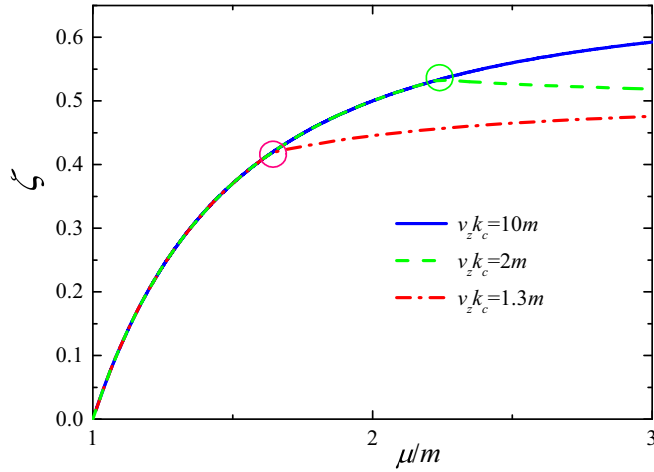


FIG. 3. Parameter ζ as a function of chemical potential μ for different values of the Brillouin zone size $v_z k_c$. Red and green circles show the point of the Lifshitz transition for $v_z k_c = 1.3$ and 2 , respectively.

The anomalous Green's function looks quite complex. However, only the $\tilde{f}(k, \Delta, \omega)$ part of the anomalous Green's function contributes to the integral over the Brillouin zone

$$\tilde{f}(k, \Delta, \omega) = -m\omega(\Delta_x s_x + \Delta_y s_y)\sigma_x + (\Delta_x s_x \sigma_y + \Delta_y s_y \sigma_y) \times (m^2 - \mu^2 - \omega^2 - v_z^2 k_z^2)/2. \quad (20)$$

The self-consistent equation for the nematic order parameter $\Delta_i = -gT/4 \sum_{\omega, k} \text{Tr}[\sigma_y s_i F_0]$, $i = x, y$ is written as

$$\Delta_{x(y)} = -gT \sum_{\omega} \int \frac{d^3 k}{(2\pi)^3} \Delta_{x(y)} \times \frac{(m^2 - \mu^2 - \omega^2 - v_z^2 k_z^2)}{(m^2 + v_z^2 k_z^2 + v^2(k_x^2 + k_y^2) - \mu^2 + \omega^2)^2 + 4\mu^2 \omega^2}, \quad (21)$$

where g is the coupling strength. Different orientations of the nematicity (or even any superposition of Δ_x and Δ_y) have the same T_c . So, we can consider only one orientation of the nematicity Δ_x without loss of generality. We can see from this expression that momentum along the z direction has a distinct impact on the value of the critical temperature. Integration over the momentum gives us

$$\Delta = \frac{\pi g T \rho(\mu)}{4} \zeta \sum_{\omega} \frac{\Delta}{|\omega|}, \quad (22)$$

where we introduce parameter ζ as

$$\zeta = \frac{(1 + r_L^2/3)(\mu^2 - m^2)}{2\mu^2}. \quad (23)$$

In a weak coupling approximation critical temperature expresses as $T_{c0} \simeq 1.14\omega_D \exp[-4/g\zeta\rho(\mu)]$, where ω_D is the Debye cutoff. We see that this expression is identical to the expression for the critical temperature of the s -wave superconductor with the renormalized by ζ coupling strength. We plot parameter ζ as a function of the chemical potential for different values of the Brillouin zone cutoff k_c in Fig. 3. We see that after the Lifshitz transition parameter ζ has slow

growth in comparison with the case of closed Fermi surface and can even decrease with the increase of the chemical potential. In case of closed Fermi surface $r_L = 1$ we have $\zeta = 2/3(1 - m^2/\mu^2)$ while cylindrical one $r_L = 0$ gives us a smaller value $\zeta = 1/2(1 - m^2/\mu^2)$.

IV. EFFECTS OF SCALAR IMPURITIES

In this section we study the effects of random charged impurities. We will describe disorder by a potential $V_{\text{imp}} = u_0 \tau_z \sum_i \delta(\mathbf{r} - \mathbf{R}_i)$, where $\delta(\mathbf{r})$ is the Dirac delta function, \mathbf{R}_j are the positions of the randomly distributed pointlike impurities with the local potential u_0 and concentration n_i , and τ_z shows that electrostatic potential acts contrary on electrons and holes. We assume that the disorder is Gaussian, that is, $\langle V_{\text{imp}} \rangle = 0$ and $\langle V_{\text{imp}}(\mathbf{r}_1) V_{\text{imp}}(\mathbf{r}_2) \rangle = n_i u_0^2 \delta(\mathbf{r}_1 - \mathbf{r}_2)$.

Self-energy is calculated as

$$\hat{\Sigma} = n_i u_0^2 \sum_k \tau_z \hat{G} \tau_z, \quad (24)$$

and has the following matrix structure:

$$\hat{\Sigma} = \begin{pmatrix} \Sigma_e & \Sigma_F \\ \bar{\Sigma}_F & \Sigma_h \end{pmatrix}. \quad (25)$$

We calculate self-energy of the normal state in a first Born approximation as

$$\Sigma_{e(h)} = n_i u_0^2 \sum_k G_{0e(h)}. \quad (26)$$

Self-energy of the normal part has two components due to strong hybridization between orbitals [44]. We assume that Debye cutoff is small $\omega_D \ll \sqrt{\mu^2 - m^2}$ and calculate self-energies at infinitesimally small frequency $\Sigma_e(\omega) = \Sigma_e(\omega \rightarrow 0)$ that means that we keep only the imaginary part of the self-energy. The real part of the self-energy leads to a small addition to μ and m which we can neglect. Under this assumption self-energy of the normal state is

$$\Sigma_{e(h)}(\omega) = \Sigma_{e(h)0} + \Sigma_{e(h)m} \sigma_z, \quad (27)$$

$$\Sigma_{e(h)0}(\omega) = -i\Gamma_0, \quad \Sigma_{e(h)m}(\omega) = -i\Gamma_z, \quad (28)$$

$$\Gamma_0 = \text{sgn}(\omega) n_i u_0^2 \frac{\pi \rho(\mu)}{4}, \quad \Gamma_z = \Gamma_0 \frac{m}{\mu}. \quad (29)$$

Disorder-averaged Green's function of the normal state $G_{e(h)}$ can be found using the Dyson equation $G_{e(h)}^{-1} = G_{0e(h)}^{-1} - \Sigma_{e(h)}$. This results in renormalization of the Matsubara frequency $\omega \rightarrow \omega + \Gamma_0$ and single-electron gap $m \rightarrow m - i\Gamma_z$.

We calculate anomalous self-energy using disorder-averaged Green's functions of the normal state as

$$\Sigma_F = -n_i u_0^2 \sum_k G_e \hat{\Delta} G_h. \quad (30)$$

Here the ‘‘minus’’ sign appears due to τ_z factor in the impurity potential that appears due to different charges of electrons and holes. Anomalous self-energy has two components:

$$\Sigma_F = (\Delta_x s_x + \Delta_y s_y)(\sigma_y \Sigma_{F1} + \sigma_x \Sigma_{F2}), \quad (31)$$

$$\Sigma_{F1}(\omega) = \bar{\Gamma} \zeta / \omega, \quad \Sigma_{F2}(\omega) = \bar{\Gamma} \frac{m}{\mu^2}.$$

Here $\bar{\Gamma} = \Gamma_0(1 + m^2/\mu^2)$ is the effective scattering rate and parameter ζ is defined by Eq. (23). As we can see, Σ_{F1} renormalizes the value of the order parameter $\hat{\Delta}$, while Σ_{F2} brings a new term $i\sigma_z \hat{\Delta}$. In general, this means that the ground state is a mixture between spontaneously generated order parameter $\hat{\Delta}$ and disorder-induced term $i\sigma_z \hat{\Delta}$. However, this new term

is small since $\Sigma_{F1} \propto 1/|\omega|$ and $\Sigma_{F2} \propto m/\mu^2$. Thus, in case of $\omega_D/\mu \ll 1$ the ground state has only component $\hat{\Delta}$ in the order parameter.

Disorder-averaged anomalous Green's functions is calculated as $F = G_e(\hat{\Delta} + \Sigma_F)G_h$. Self-consistent equation $\Delta_i = -gT/4 \sum_{\omega,k} \text{Tr}[\sigma_y s_i F]$ leads to

$$\Delta_{x(y)} = -gT \sum_{\omega} \int \frac{d^3k}{(2\pi)^3} \frac{\Delta_{x(y)}[1 + \Sigma_{F1}(\omega)][m^2 - \mu^2 - (\omega + \Gamma_0)^2 + \Gamma_z^2 - v_z^2 k_z^2] + 2\Sigma_{F2}(\omega)(m\omega - \Gamma_z \mu + m\Gamma_0)}{[m^2 + v_z^2 k_z^2 + v^2(k_x^2 + k_y^2) - \mu^2 + (\omega + \Gamma_0)^2 - \Gamma_z^2]^2 + 4[\mu(\omega + \Gamma_0) + m\Gamma_z]^2}. \quad (32)$$

For weak scattering $|\Gamma_0|, |\Gamma_z| \ll \mu$ and $\omega_D \ll \mu$ we calculate to

$$\Delta = \frac{\pi g \zeta \rho(\mu) T}{4} \sum_{\omega} \frac{\tilde{\Delta}}{|\tilde{\omega}|}, \quad (33)$$

where renormalized by the disorder Matsubara frequency $\tilde{\omega}$ and order parameter $\tilde{\Delta}$ are

$$\tilde{\omega} = \omega + \bar{\Gamma}, \quad \tilde{\Delta} = \Delta \left(1 + \frac{\bar{\Gamma} \zeta}{\omega}\right). \quad (34)$$

If we substitute $\tilde{\omega}$ and $\tilde{\Delta}$ back into the equation for the anomalous Green's function F we arrive to the different $\tilde{\Delta}$. Self-consistent procedure leads to $\tilde{\Delta}$ in the following equations:

$$\tilde{\omega} = \omega + \bar{\Gamma}, \quad \tilde{\Delta} = \Delta + \tilde{\Delta} \bar{\Gamma} \zeta / \tilde{\omega} \quad (35)$$

or

$$\tilde{\omega} = \omega + \bar{\Gamma}, \quad \tilde{\Delta} = \Delta / (1 - \bar{\Gamma} \zeta / \tilde{\omega}). \quad (36)$$

The self-consistent equation in a self-consistent approximation is written as

$$\Delta = \frac{\pi g \rho(\mu) \zeta T}{4} \sum_{\omega} \frac{\Delta}{|\omega + (1 - \zeta) \bar{\Gamma}|}. \quad (37)$$

This equation leads to the Abrikosov-Gor'kov equation for a critical temperature

$$\ln \frac{T_c}{T_{c0}} = \Psi(1/2) - \Psi\left(1/2 + \frac{\bar{\Gamma}(1 - \zeta)}{2\pi T_c}\right), \quad (38)$$

where $\Psi(x)$ is the digamma function. Critical temperature is completely suppressed at

$$(1 - \zeta) \bar{\Gamma}_c = 0.88 T_{c0}. \quad (39)$$

Nematic superconductivity is suppressed by the large disorder that confirms results of Refs. [27–29]. The critical temperature depends on the parameter ζ that determines both the critical temperature in a clean case and robustness against the disorder according to Eqs. (22) and (37). This parameter depends on the shape of the Fermi surface as it is shown in Fig. 4. The closed Fermi surface $r_L = 1$ gives $\zeta = \frac{2}{3}$ for $\mu \gg m$ that is consistent with the results of Ref. [27]. Cylindrical Fermi surface $r_L = 0$ gives $\zeta = \frac{1}{2}$. It means that a closed Fermi surface is more robust against the disorder and has a higher critical temperature for the same density of states than a cylindrical one.

V. SPECTRAL REPRESENTATION

In order to get inside how parameter ζ ties together both critical temperature and robustness against the disorder we write Gor'kov equations in a spectral representation. We suppose that matrix \hat{A} determines spin and orbital structures of the order parameter $\hat{\Delta} = \Delta \hat{A}$ where Δ is the scalar that determines the value of the order parameter and $\hat{A}^\dagger \hat{A} = 1$. \hat{A} is the $n \times n$ matrix where n is the number of bands that contribute to the order parameter. We consider the case when only a single band of the normal state ϵ_l crosses Fermi level μ . We consider that this band is degenerate p_l times $H_N \psi_i = \epsilon_l \psi_i$, $i \in \mathbf{p}_l = 1, \dots, p_l$, where \mathbf{p}_l denotes the set of eigenvectors with energy ϵ_l . We also assume the presence of the time-reversal symmetry. Green's function in a normal state and anomalous Green's function are given by [27]

$$G_{e0} = \sum_j \frac{P_j}{i\omega + \mu - \epsilon_j}, \quad G_{h0} = \sum_j \frac{P_j}{i\omega - \mu + \epsilon_j}, \quad (40)$$

$$F_0 = \Delta \sum_{i,j} \frac{P_i \hat{A} P_j}{(i\omega + \mu - \epsilon_i)(i\omega - \mu + \epsilon_j)}, \quad (41)$$

where the projector on the band with energy ϵ_i is given by $P_i = |\psi_i\rangle\langle\psi_i|$. Using the assumption that only the level with the energy ϵ_l crosses the Fermi level, the self-consistent equation for the value of the order parameter Δ in a clean limit is

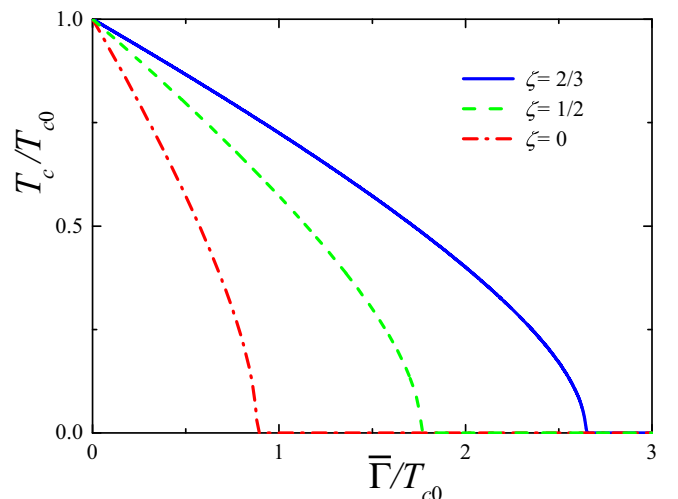


FIG. 4. Critical temperature T_c as a function of disorder $\bar{\Gamma}$ for different values of parameter ζ .

TABLE I. Superconducting fitness function F_c and parameter ζ for possible odd-parity superconducting pairings taken from Ref. [1]. Here $\langle \dots \rangle$ means average over the Fermi surface of the normal state.

	$\hat{\Delta}_2$	$\hat{\Delta}_3$	$\hat{\Delta}_4$
Representation	A_{1u}	A_{2u}	E_u
Matrix structure \hat{A}	$\sigma_y s_z$	σ_z	$(\sigma_y s_x, \sigma_y s_y)$
$F_c/2i$	$R_1 \sigma_z - m \sigma_x s_z$	$v_z k_z \sigma_x - v(k_y s_x - k_x s_y) \sigma_y - R_1 s_z \sigma_y$	$(v k_y \sigma_z - m \sigma_x s_x, -v k_x \sigma_z - m \sigma_x s_y)$
ζ	$\langle \frac{v_z^2 k_z^2 + v^2 k_x^2 + v^2 k_y^2}{\mu^2} \rangle$	$\langle \frac{m^2}{\mu^2} \rangle$	$(\langle \frac{m^2 + v^2 k_x^2 + R_1^2}{\mu^2} \rangle, \langle \frac{m^2 + v^2 k_y^2 + R_1^2}{\mu^2} \rangle)$

written as

$$\Delta = -\frac{gT}{n} \sum_{\omega, k} \text{Tr}[\hat{A}^\dagger F_0] = \frac{\pi g \rho(\mu)}{n} \zeta \sum_{\omega} \frac{\Delta}{|\omega|}. \quad (42)$$

Here density of states $\rho(\mu) = \omega p_l / \pi \sum_k 1/[\omega^2 + (\epsilon_l - \mu)^2]$ at $\omega \rightarrow +0$. Parameter ζ expresses through the Fermi surface the projected order parameter A_p as

$$\zeta = \text{Tr}\langle A_p^\dagger A_p \rangle_{\text{FS}} / p_l, \quad (43)$$

$$A_{pij} = \langle \psi_i | \hat{A} | \psi_j \rangle, \quad (44)$$

where A_{pij} is calculated for the states with eigenenergy that cross the Fermi level $i, j \in \mathbf{p}_l$. Similar expression can be obtained through direct calculation of the Cooper susceptibility for the general case of momentum-dependent order parameter $A = A_k$ [45].

If we neglect scattering between the different states within the band then self-energy of the normal state in presence of scalar disorder is diagonal $\Sigma_N = -i\Gamma_0 \hat{1}$ where $\Gamma_0 = \text{sgn}(\omega) n_i u_0^2 \pi \rho / n$. The Dyson equation for the normal state $G_N^{-1} = G_{N0}^{-1} - \Sigma_N$ shows that disorder renormalizes Matsubara frequency $\omega \rightarrow \tilde{\omega} = \omega + \Gamma_0$.

The leading contribution of the anomalous self-energy $\Sigma_F = -n_i u_0^2 \sum_k F_0(\tilde{\omega})$ that renormalizes the value of the order parameter is

$$\Sigma_F = \sigma_F \hat{A}^\dagger, \quad (45)$$

$$\sigma_F = -n_i u_0^2 \Delta \sum_k \text{Tr}[\hat{A}^\dagger F_0] / n = \Delta \zeta \Gamma_0 / \omega. \quad (46)$$

From the Dyson equation $G^{-1} = G_0^{-1} - \Sigma$ we can see that in presence of the disorder the anomalous Green's function given by Eq. (40) can be obtained by the substitution $\hat{\Delta} \rightarrow \tilde{\Delta} + \Sigma_F$. As a result, the self-consistent equation is

$$\Delta = \pi g \zeta \rho / n \sum_{\omega} \frac{\tilde{\Delta}}{|\tilde{\omega}|}, \quad (47)$$

where

$$\tilde{\omega} = \omega + \Gamma_0, \quad \tilde{\Delta} = \Delta + \Delta \zeta \Gamma_0 / \omega. \quad (48)$$

Self-consistent procedure leads to

$$\tilde{\omega} = \omega + \Gamma_0, \quad \tilde{\Delta} = \Delta + \tilde{\Delta} \zeta \Gamma_0 / \omega, \quad (49)$$

and we arrived to the expression

$$\Delta = -\frac{gT}{n} \sum_{\omega, k} \text{Tr}[\hat{A}^\dagger F] = \frac{\pi g \zeta \rho}{n} \sum_{\omega} \frac{\Delta}{|\omega + (1 - \zeta)\Gamma_0|}, \quad (50)$$

which is similar to Eq. (37) up to substitution $\Gamma_0 \rightarrow \tilde{\Gamma}$ and $n \rightarrow 4$. We have shown that correspondence between critical temperature and robustness against the disorder is the general feature of the superconductivity.

The superconducting fitness function in case of the system with time-reversal symmetry is written as $F_c = [H_N, A]$ (see Ref. [46]). We rewrite the fitness function $F_c = \sum F_{ci}$ in a spectral representation where $F_{ci} = \epsilon_i [P_i, A]$. We introduce partial fitness function $F_{pc} = \sum F_{ci}$ where the sum $i \in \mathbf{p}_l$ is taken over the states that correspond to band with the energy ϵ_i that crosses the Fermi level. The expression $\text{Tr}(F_{pc}^\dagger F_{pc}) / \epsilon_i = 1 - \zeta$ establishes a connection between superconducting fitness F_c and parameter ζ . If the superconducting state is perfectly fit $F_c = 0$ then the parameter $\zeta = 1$ that ensures robustness against the disorder [30,47]. This case can happen if the Hamiltonian of the normal state commutes with the matrix structure of the order parameter $[H_N, A] = 0$. The s -wave order parameter $\hat{A} = \hat{1}$ always satisfies this condition that leads to the Anderson theorem [21]. If the matrix structure of the superconducting order parameter is the integral of motion, then this superconductivity is also robust against the disorder [48].

Parameter ζ is a useful quantity: it shows how the symmetry of the order parameter affects its critical temperature and its robustness against the disorder. We calculate parameter ζ along with the superconducting fitness function F_c for different possible odd-parity superconducting order parameters for the topological insulator with the hexagonal warping $H_N + R_1 s_z \sigma_z$ where $R_1 = \lambda k_x (k_x^2 - 3k_y^2)$. Results are summarized in Table I. Terms that contribute to the superconducting fitness F_c decrease the critical temperature of the corresponding order parameter. We see that large single-electron gap m disfavors Δ_2 and nematic Δ_4 order parameters and stimulates Δ_3 . Hexagonal warping stimulates nematic superconductivity [49] Δ_4 that allows it to win against Δ_2 . This analysis is similar to the one from Ref. [46]. Parameter ζ as a function of the Lifshitz transition parameter r_L for Δ_2 and Δ_4 order parameters is shown in Fig. 5. We see that ζ decreases with the transformation of the Fermi surface from closed one to cylindrical for both states. At some point, the Lifshitz transition makes critical temperature for Δ_4 higher than Δ_2 . This effect occurs due to an effective increase of warping for an open Fermi surface. Thus, we conclude that the Lifshitz transition helps the nematic state to compete against other odd-parity order parameters. However, the Lifshitz transition decreases parameter ζ for the nematic state while for the s -wave order parameter this quantity is unaffected. Thus, the open Fermi surface helps the s -wave order parameter the most.

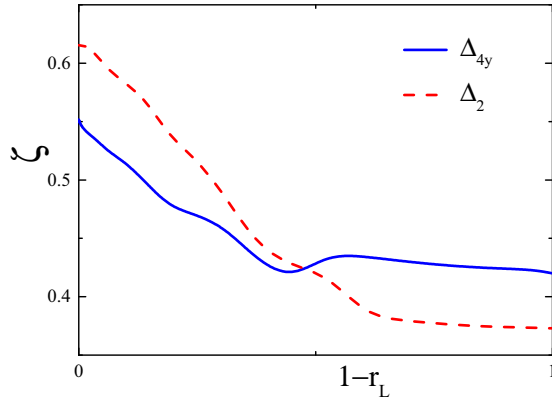


FIG. 5. Parameter ζ as a function of Lifshitz parameter r_L for nematic state Δ_4 and state Δ_2 .

VI. MEISSNER CURRENT

In this section we show how disorder and shape of the Fermi surface affect Meissner current in the nematic superconductor. The superconducting current in a linear response is proportional to the vector potential and superconducting density $J_\alpha = -n_s A_\alpha$. We express the current operator as $J_\alpha = -\sum_\beta K_{\alpha\beta} A_\beta$ where the Meissner kernel is [50]

$$K_{\alpha\beta} = -T \sum_{k,\omega} v_\alpha F v_\beta \bar{F}. \quad (51)$$

The current operator $v_\alpha = -\partial H_N(k_\alpha - A_\alpha)/\partial A_\alpha = \partial H_N(k_\alpha)/\partial k_\alpha$ coincides with the velocity operator in case of linear spectrum $\alpha = x, y, z$. In general, we should use full Green's function \hat{G} in Eq. (51) and then subtract the contribution of the normal part. In our case of linearized Green's functions, it means that we keep the anomalous part of Green's function only. As it is shown in Ref. [50] this procedure is correct even if we calculate response beyond linearized in $\hat{\Delta}$ theory.

First, we compute the correlation function in a clean limit near the critical temperature using Eq. (19) for the anomalous Green's function. We consider only Δ_x orientation. Straightforward calculations give us the following expressions:

$$K_{xx} = \frac{45 - 10r_L^2 - 3r_L^4}{32} K_0, \quad (52)$$

$$K_{yy} = \frac{15 + 10r_L^2 - 9r_L^4}{32} K_0,$$

$$K_{zz} = \frac{v_z^2 r_L^2 (5 + 3r_L^2)}{8v^2} K_0.$$

$$K_0 = \frac{v^2 \pi \rho(\mu) (1 - m^2/\mu^2)^2}{15} T \sum_\omega \Delta^2 / |\omega|^3. \quad (53)$$

Integration over the Matsubara frequencies gives us $K_0 = \kappa \Delta^2 / T^2$ where $\kappa = v^2 \rho(\mu) (1 - m^2/\mu^2)^2 7\zeta(3) / 120\pi^2$. Here $\zeta(3) \simeq 1.2$ is the Riemann zeta function. In case of $r_L = 1$ for closed Fermi surface we get $K_{xx} = 2K_{yy} = K_{zz} v_z^2 / v^2 = K_0(\omega)$ which is similar to the results of Ref. [50]. In case of $r_L = 0$ for cylindrical Fermi surface we have $K_{xx} = 3K_{yy} = 3K_0(\omega)$ and $K_{zz} = 0$. We plot correlation functions $K_{\alpha\alpha}$ as a function of the parameter of the Lifshitz

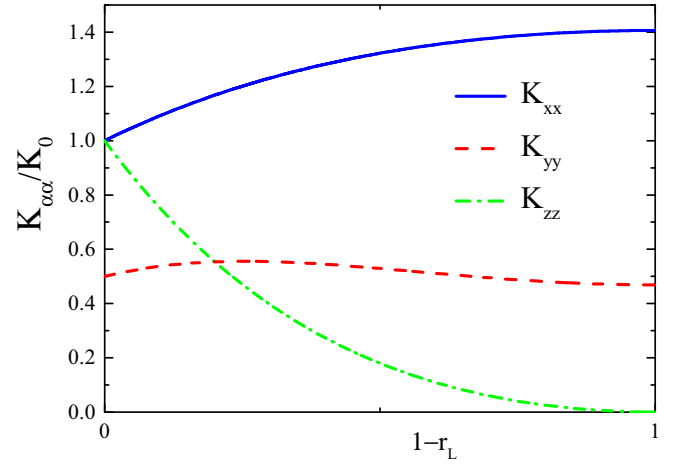


FIG. 6. Meissner kernels $K_{\alpha\alpha}$ as functions of Lifshitz parameter r_L for Δ_x nematicity direction.

transition r_L in Fig. 6 for $v_z/v = \frac{2}{3}$. We see that the Lifshitz transition increases anisotropy of the response.

We can introduce disorder by substitution $\omega \rightarrow \tilde{\omega}$ and $\Delta \rightarrow \tilde{\Delta}$, where $\tilde{\omega}$ and $\tilde{\Delta}$ are determined by Eq. (36). Inserting this into Eq. (53) gives us the following expression for the Meissner kernel \tilde{K}_0 in disordered case:

$$\tilde{K}_0 = \kappa \sum_\omega \frac{\Delta^2}{(\omega + \bar{\Gamma})[\omega + \bar{\Gamma}(1 - \zeta)]^2}. \quad (54)$$

We can see from this expression that superconducting density is suppressed by the disorder even if the critical temperature is robust $\zeta = 1$. In case of $\bar{\Gamma} \ll T_c \ll \bar{\Gamma}/(1 - \zeta)$ critical temperature is unaffected by the disorder while Meissner currents are suppressed $\tilde{K} \propto 1/\bar{\Gamma}$. In case of large disorder $T_c \ll \bar{\Gamma}/(1 - \zeta)$ superconducting density is suppressed because of the suppression of the critical temperature by the disorder $\tilde{K} \propto \Delta^2 \propto T_c - T$. We plot the Meissner kernel as a function of disorder in Fig. 7. We see that the superconducting

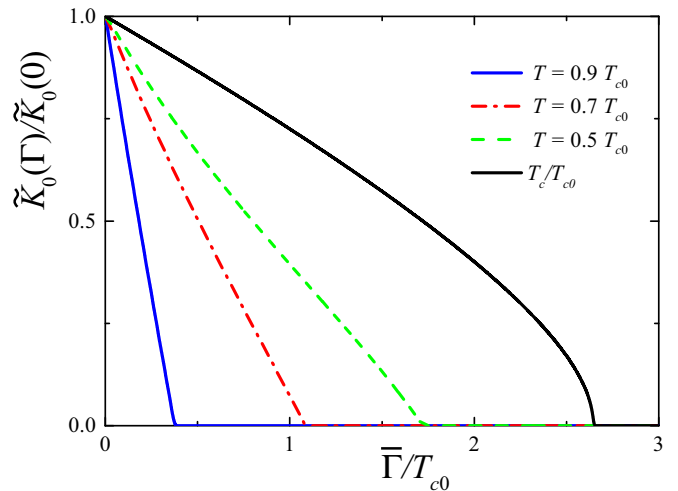


FIG. 7. Meissner kernel \tilde{K}_0 as function of disorder $\bar{\Gamma}/T_{c0}$ for different values of temperature T for $\zeta = \frac{2}{3}$. Black line corresponds to the dependence of the critical temperature T_c from the disorder $\bar{\Gamma}$.

density is suppressed stronger than the critical temperature. Anisotropy of the Meissner currents remains the same as in the clean case.

VII. DISCUSSION

In Ref. [39] the authors state that the superconductivity in doped topological insulators appears along with the Lifshitz transition from closed to open Fermi surface. The open Fermi surface has been observed in different compounds of doped topological insulators with nematic superconductivity [38,51,52]. In our work, we get that the Lifshitz transition is destructive for nematic superconductivity. Both critical temperature and robustness against the disorder are smaller for the open Fermi surface than for the closed one if the density of states is the same. This connection between the shape of the Fermi surface and superconducting properties can be one of the reasons why the critical temperature in doped topological insulators is insensitive to the carrier density [52].

Nematic superconductivity is only partially robust against potential disorder and is suppressed if the disorder is large. Our results are consistent with Refs. [27–29] and are in disagreement with Ref. [30]. We derive that critical temperature in the clean case and robustness against disorder are closely tied. The connection between these quantities comes from the mutual symmetry between the Hamiltonian of the normal state and the spin-orbital structure of the superconducting order parameter. We express this connection through superconducting order parameter that is projected onto the states of the Hamiltonian of the normal state [see Eq. (43)]. This quantity is closely tied with the conception of the superconducting fitness [46] (see Sec. V). A similar connection between robustness against the disorder and superconducting fitness has been derived for the s -wave states [27]. In Refs. [30,47] connection between superconducting fitness and robustness against the disorder has been discussed as well.

In Ref. [25] Cu-doped Bi_2Se_3 samples show twofold behavior of the second critical field that is a distinctive feature of the nematic superconductivity [25]. At large doping, carrier density substantially increases and twofold symmetry of the second critical field H_{c2} disappears. It was suggested that this occurs due to phase transition to the different superconducting states. An increase of the chemical potential gradually transforms the Fermi surface into the cylindrical one. This process makes the nematic superconducting state less favorable in comparison with the even-parity s -wave superconducting state. Thus, we conclude that the most likely superconducting state in Cu-overdoped Bi_2Se_3 without twofold symmetry of H_{c2} is even-parity s wave.

We found that the Meissner current near the critical temperature is diamagnetic and anisotropic that confirms the results of Ref. [50]. The Meissner current is largest along

the nematicity direction for the closed Fermi surface. This anisotropy is increased by the Lifshitz transition $K_{xx} = 3K_{yy}$ for $r_L = 0$. In general, anisotropic superconductors have quite complex behavior in a magnetic field [53]. We assume a simplified situation that London penetration length for the magnetic field applied along the i direction expresses through the Meissner kernel $\lambda_i^2 \propto 1/K_{ii}$ as for the isotropic superconductor. We are not aware of the works on the in-plane anisotropy of the first critical field, so we focus on the anisotropy between averaged in-plane $\lambda_{ab}^2 = (\lambda_x^2 + \lambda_y^2)/2$ and out-of-plane penetration lengths $\lambda_c^2 = \lambda_z^2$ that is $\kappa = \lambda_c^2/\lambda_{ab}^2$. We take $v_z/v = \frac{2}{3}$ from Ref. [41]. In case of closed Fermi surface our calculations lead to $\kappa = \frac{1}{2}$ for $v_z/v = \frac{2}{3}$. In Ref. [3] this anisotropy parameter $\kappa \simeq 2.4$ while in Ref. [33] $\kappa \simeq 2.6$. As we can see, the assumption of a closed Fermi surface is inconsistent with the experimental results. We found that $r_L \sim \frac{1}{2}$ gives experimentally relevant anisotropy of the first critical field. In this case, the Fermi surface is a corrugated cylinder.

In Ref. [24] it was obtained that the superconducting density is suppressed by the disorder while the critical temperature is largely unaffected. In Ref. [23] the authors conclude that only a small part of scattering events contribute to the depairing of Cooper pairs. This situation occurs since critical temperature T_c is suppressed by effective disorder $(1 - \zeta)\bar{\Gamma}$ and only $1 - \zeta$ of scattering events contribute to the depairing. However, every scattering event contributes to the suppression of the superconducting density similar to the case of s -wave superconductor [31]. Thus, superconducting density is suppressed stronger by the disorder than the critical temperature.

In general, strong Coulomb repulsion that is accompanied by the fluctuations in E_u channel can lead to the mixing between singlet s -wave order parameter and triplet nematic order parameter within E_u representation [54]. However, due to large dielectric constant Coulomb repulsion is weak in topological insulators. Note that presence of the fluctuations E_u only does not lead to such coupling [55].

In conclusion, we get that Lifshitz transition from closed to open Fermi surface affects both critical temperature and robustness against the disorder in nematic superconductors. We found that critical temperature in a clean limit and robustness against the disorder are tied through the superconducting fitness. Anisotropy of Meissner currents is increased by the Lifshitz transition.

ACKNOWLEDGMENTS

We acknowledge support by the Russian Science Foundation under Grant No. 20-72-00030 and partial support from the Foundation for the Advancement of Theoretical Physics and Mathematics “BASIS.”

- [1] L. Fu and E. Berg, Odd-Parity Topological Superconductors: Theory and Application to $\text{Cu}_x\text{Bi}_2\text{Se}_3$, *Phys. Rev. Lett.* **105**, 097001 (2010).
 [2] S. Yonezawa, Nematic superconductivity in doped Bi_2Se_3 topological superconductors, *Condensed Matter* **4**, 2 (2018).

- [3] K. Matano, M. Kriener, K. Segawa, Y. Ando, and G. qing Zheng, Spin-rotation symmetry breaking in the superconducting state of $\text{Cu}_x\text{Bi}_2\text{Se}_3$, *Nat. Phys.* **12**, 852 (2016).
 [4] Y. Pan, A. M. Nikitin, G. K. Araizi, Y. K. Huang, Y. Matsushita, T. Naka, and A. de Visser, Rotational symmetry breaking in the

- topological superconductor $\text{Sr}_x\text{Bi}_2\text{Se}_3$ probed by upper-critical field experiments, *Sci. Rep.* **6**, 28632 (2016).
- [5] A. Y. Kuntsevich, M. A. Bryzgalov, V. A. Prudkoglyad, V. P. Martovitskii, Y. G. Selivanov, and E. G. Chizhevskii, Structural distortion behind the nematic superconductivity in $\text{Sr}_x\text{Bi}_2\text{Se}_3$, *New J. Phys.* **20**, 103022 (2018).
- [6] A. Y. Kuntsevich, M. A. Bryzgalov, R. S. Akzyanov, V. P. Martovitskii, A. L. Rakhmanov, and Y. G. Selivanov, Strain-driven nematicity of odd-parity superconductivity in $\text{Sr}_x\text{Bi}_2\text{Se}_3$, *Phys. Rev. B* **100**, 224509 (2019).
- [7] T. Asaba, B. J. Lawson, C. Tinsman, L. Chen, P. Corbae, G. Li, Y. Qiu, Y. S. Hor, L. Fu, and L. Li, Rotational Symmetry Breaking in a Trigonal Superconductor Nb-Doped Bi_2Se_3 , *Phys. Rev. X* **7**, 011009 (2017).
- [8] L. Fu, Odd-parity topological superconductor with nematic order: Application to $\text{Cu}_x\text{Bi}_2\text{Se}_3$, *Phys. Rev. B* **90**, 100509(R) (2014).
- [9] J. W. F. Venderbos, V. Kozii, and L. Fu, Identification of nematic superconductivity from the upper critical field, *Phys. Rev. B* **94**, 094522 (2016).
- [10] T. H. Hsieh and L. Fu, Majorana Fermions and Exotic Surface Andreev Bound States in Topological Superconductors: Application to $\text{Cu}_x\text{Bi}_2\text{Se}_3$, *Phys. Rev. Lett.* **108**, 107005 (2012).
- [11] L. Hao and T.-K. Lee, Effective low-energy theory for superconducting topological insulators, *J. Phys.: Condens. Matter* **27**, 105701 (2015).
- [12] L. Hao and C. S. Ting, Nematic superconductivity in $\text{Cu}_x\text{Bi}_2\text{Se}_3$: Surface Andreev bound states, *Phys. Rev. B* **96**, 144512 (2017).
- [13] A. A. Zyuzin, J. Garaud, and E. Babaev, Nematic Skyrmions in Odd-Parity Superconductors, *Phys. Rev. Lett.* **119**, 167001 (2017).
- [14] P. T. How and S.-K. Yip, Half quantum vortices in a nematic superconductor, *Phys. Rev. Research* **2**, 043192 (2020).
- [15] F. Wu and I. Martin, Majorana Kramers pair in a nematic vortex, *Phys. Rev. B* **95**, 224503 (2017).
- [16] R. S. Akzyanov, A. V. Kapranov, and A. L. Rakhmanov, Spontaneous strain and magnetization in doped topological insulators with nematic and chiral superconductivity, *Phys. Rev. B* **102**, 100505(R) (2020).
- [17] M. Hecker and J. Schmalian, Vestigial nematic order and superconductivity in the doped topological insulator $\text{Cu}_x\text{Bi}_2\text{Se}_3$, *npj Quantum Mater.* **3**, 26 (2018).
- [18] H. Uematsu, T. Mizushima, A. Tsuruta, S. Fujimoto, and J. A. Sauls, Chiral Higgs Mode in Nematic Superconductors, *Phys. Rev. Lett.* **123**, 237001 (2019).
- [19] W.-C. Bao, Q.-K. Tang, D.-C. Lu, and Q.-H. Wang, Visualizing the d vector in a nematic triplet superconductor, *Phys. Rev. B* **98**, 054502 (2018).
- [20] D. Khokhlov and R. Akzyanov, Quasiparticle interference in doped topological insulators with nematic superconductivity, *Physica E* **133**, 114800 (2021).
- [21] P. Anderson, Theory of dirty superconductors, *J. Phys. Chem. Solids* **11**, 26 (1959).
- [22] A. J. Millis, S. Sachdev, and C. M. Varma, Inelastic scattering and pair breaking in anisotropic and isotropic superconductors, *Phys. Rev. B* **37**, 4975 (1988).
- [23] M. P. Smylie, K. Willa, H. Claus, A. Snezhko, I. Martin, W.-K. Kwok, Y. Qiu, Y. S. Hor, E. Bokari, P. Niraula, A. Kayani, V. Mishra, and U. Welp, Robust odd-parity superconductivity in the doped topological insulator $\text{Nb}_x\text{Bi}_2\text{Se}_3$, *Phys. Rev. B* **96**, 115145 (2017).
- [24] M. Kriener, K. Segawa, S. Sasaki, and Y. Ando, Anomalous suppression of the superfluid density in the $\text{Cu}_x\text{Bi}_2\text{Se}_3$ superconductor upon progressive Cu intercalation, *Phys. Rev. B* **86**, 180505(R) (2012).
- [25] T. Kawai, C. G. Wang, Y. Kandori, Y. Honoki, K. Matano, T. Kambe, and G. Qing Zheng, Direction and symmetry transition of the vector order parameter in topological superconductors $\text{Cu}_x\text{Bi}_2\text{Se}_3$, *Nat. Commun.* **11**, 235 (2020).
- [26] Y. Nagai, Robust superconductivity with nodes in the superconducting topological insulator $\text{Cu}_x\text{Bi}_2\text{Se}_3$: Zeeman orbital field and nonmagnetic impurities, *Phys. Rev. B* **91**, 060502(R) (2015).
- [27] D. C. Cavanagh and P. M. R. Brydon, Robustness of unconventional s -wave superconducting states against disorder, *Phys. Rev. B* **101**, 054509 (2020).
- [28] D. Dentelski, V. Kozii, and J. Ruhman, Effect of interorbital scattering on superconductivity in doped Dirac semimetals, *Phys. Rev. Research* **2**, 033302 (2020).
- [29] T. Sato and Y. Asano, Superconductivity in Cu-doped Bi_2Se_3 with potential disorder, *Phys. Rev. B* **102**, 024516 (2020).
- [30] L. Andersen, A. Ramires, Z. Wang, T. Lorenz, and Y. Ando, Generalized Anderson's theorem for superconductors derived from topological insulators, *Sci. Adv.* **6**, eaay6502 (2020).
- [31] L. S. Levitov and A. V. Shtyov, *Green's Functions. Theory and Practice* (MIT Press, Cambridge, MA, 2002).
- [32] M. P. Smylie, H. Claus, U. Welp, W.-K. Kwok, Y. Qiu, Y. S. Hor, and A. Snezhko, Evidence of nodes in the order parameter of the superconducting doped topological insulator $\text{Nb}_x\text{Bi}_2\text{Se}_3$ via penetration depth measurements, *Phys. Rev. B* **94**, 180510(R) (2016).
- [33] Y. Fang, W.-L. You, and M. Li, Unconventional superconductivity in $\text{Cu}_x\text{Bi}_2\text{Se}_3$ from magnetic susceptibility and electrical transport, *New J. Phys.* **22**, 053026 (2020).
- [34] I. M. Lifshitz, Anomalies of electron characteristics of a metal in the high pressure region, *Zh. Eksp. Teor. Fiz.* **38**, 1569 (1960) [*Sov. Phys. JETP* **11**, 1130 (1960)].
- [35] M. R. Norman, J. Lin, and A. J. Millis, Lifshitz transition in underdoped cuprates, *Phys. Rev. B* **81**, 180513(R) (2010).
- [36] D. LeBoeuf, N. Doiron-Leyraud, B. Vignolle, M. Sutherland, B. J. Ramshaw, J. Levallois, R. Daou, F. Laliberté, O. Cyr-Choinière, J. Chang, Y. J. Jo, L. Balicas, R. Liang, D. A. Bonn, W. N. Hardy, C. Proust, and L. Taillefer, Lifshitz critical point in the cuprate superconductor $\text{YBa}_2\text{Cu}_3\text{O}_y$ from high-field Hall effect measurements, *Phys. Rev. B* **83**, 054506 (2011).
- [37] A. Perali, D. Innocenti, A. Valletta, and A. Bianconi, Anomalous isotope effect near a 2.5 Lifshitz transition in a multi-band multi-condensate superconductor made of a superlattice of stripes, *Supercond. Sci. Technol.* **25**, 124002 (2012).
- [38] E. Lahoud, E. Maniv, M. S. Petrushevsky, M. Naamneh, A. Ribak, S. Wiedmann, L. Petaccia, Z. Salman, K. B. Chashka, Y. Dagan, and A. Kanigel, Evolution of the Fermi surface of a doped topological insulator with carrier concentration, *Phys. Rev. B* **88**, 195107 (2013).
- [39] A. Almoalem, I. Silber, S. Sandik, M. Lotem, A. Ribak, Y. Nitzav, A. Y. Kuntsevich, O. A. Sobolevskiy, Y. G. Selivanov, V. A. Prudkoglyad, M. Shi, L. Petaccia, M. Goldstein, Y. Dagan, and A. Kanigel, Link between superconductivity and a Lifshitz

- transition in intercalated Bi_2Se_3 , *Phys. Rev. B* **103**, 174518 (2021).
- [40] H. Zhang, C.-X. Liu, X.-L. Qi, X. Dai, Z. Fang, and S.-C. Zhang, Topological insulators in Bi_2Se_3 , Bi_2Te_3 and Sb_2Te_3 with a single Dirac cone on the surface, *Nat. Phys.* **5**, 438 (2009).
- [41] C.-X. Liu, X.-L. Qi, H.-J. Zhang, X. Dai, Z. Fang, and S.-C. Zhang, Model Hamiltonian for topological insulators, *Phys. Rev. B* **82**, 045122 (2010).
- [42] J. Wang, K. Ran, S. Li, Z. Ma, S. Bao, Z. Cai, Y. Zhang, K. Nakajima, S. Ohira-Kawamura, P. Cermak, A. Schneidewind, S. Y. Savrasov, X. Wan, and J. Wen, Evidence for singular-phonon-induced nematic superconductivity in a topological superconductor candidate $\text{Sr}_{0.1}\text{Bi}_2\text{Se}_3$, *Nat. Commun.* **10**, 2802 (2019).
- [43] S.-K. Yip, Models of superconducting $\text{Cu}:\text{Bi}_2\text{Se}_3$: Single- versus two-band description, *Phys. Rev. B* **87**, 104505 (2013).
- [44] R. S. Akzyanov, Bulk spin conductivity of three-dimensional topological insulators, *J. Phys.: Condens. Matter* **33**, 095701 (2020).
- [45] L. Fu, Hexagonal Warping Effects in the Surface States of the Topological Insulator Bi_2Te_3 , *Phys. Rev. Lett.* **103**, 266801 (2009).
- [46] A. Ramires, D. F. Agterberg, and M. Sigrist, Tailoring T_c by symmetry principles: The concept of superconducting fitness, *Phys. Rev. B* **98**, 024501 (2018).
- [47] E. I. Timmons, S. Teknowijoyo, M. Kończykowski, O. Cavani, M. A. Tanatar, S. Ghimire, K. Cho, Y. Lee, L. Ke, N. H. Jo, S. L. Bud'ko, P. C. Canfield, P. P. Orth, M. S. Scheurer, and R. Prozorov, Electron irradiation effects on superconductivity in PdTe_2 : An application of a generalized Anderson theorem, *Phys. Rev. Research* **2**, 023140 (2020).
- [48] K. Michaeli and L. Fu, Spin-Orbit Locking as a Protection Mechanism of the Odd-Parity Superconducting State Against Disorder, *Phys. Rev. Lett.* **109**, 187003 (2012).
- [49] R. S. Akzyanov, D. A. Khokhlov, and A. L. Rakhmanov, Nematic superconductivity in topological insulators induced by hexagonal warping, *Phys. Rev. B* **102**, 094511 (2020).
- [50] J. Schmidt, F. Parhizgar, and A. M. Black-Schaffer, Odd-frequency superconductivity and Meissner effect in the doped topological insulator Bi_2Se_3 , *Phys. Rev. B* **101**, 180512(R) (2020).
- [51] B. J. Lawson, P. Corbae, G. Li, F. Yu, T. Asaba, C. Tinsman, Y. Qiu, J. E. Medvedeva, Y. S. Hor, and L. Li, Multiple Fermi surfaces in superconducting Nb-doped Bi_2Se_3 , *Phys. Rev. B* **94**, 041114(R) (2016).
- [52] A. Y. Kuntsevich, V. P. Martovitskii, G. V. Rybalchenko, Y. G. Selivanov, M. I. Bannikov, O. A. Sobolevskiy, and E. G. Chigevskii, Superconductivity in Cu co-doped $\text{Sr}_x\text{Bi}_2\text{Se}_3$ single crystals, *Materials* **12**, 3899 (2019).
- [53] N. Kopnin, *Vortices in Type-II Superconductors Structure and Dynamics* (Oxford University Press, Oxford, 2001).
- [54] F. Wu and I. Martín, Nematic and chiral superconductivity induced by odd-parity fluctuations, *Phys. Rev. B* **96**, 144504 (2017).
- [55] V. Kozii and L. Fu, Odd-Parity Superconductivity in the Vicinity of Inversion Symmetry Breaking in Spin-Orbit-Coupled Systems, *Phys. Rev. Lett.* **115**, 207002 (2015).